ELSEVIER

Journal of Nuclear Materials 280 (2000) 186–195

journal of nuclear materials

www.elsevier.nl/locate/jnucmat

Microstructure of austenitic stainless steels irradiated at 400°C in the ORR and the HFIR spectral tailoring experiment

N. Hashimoto [a,*], E. Wakai [b], J.P. Robertson [a], T. Sawai [b], A. Hishinuma [b]

[a] *Metals and Ceramics Division, Oak Ridge National Laboratory, Building 5500 MS 6376, P.O.Box 2008, Oak Ridge, TN 37831-6376, USA*

[b] *Japan Atomic Energy Research Institute, Tokai-mura Ibaraki-ken 319-1195, Japan*

Received 8 February 2000; accepted 16 March 2000

Abstract

Microstructural evolution in solution-annealed Japanese-PCA (JPCA-SA) and four other austenitic stainless steels, irradiated at 400°C to 17.3 dpa in the ORR and the high flux isotope reactor (HFIR) spectrally tailored experiment, were investigated by transmission electron microscopy (TEM). The mean He/dpa ratio throughout the irradiation fell between 12 and 16 appm He/dpa , which is close to the He/dpa values expected for fusion. In all the specimens, a bi-modal size distribution of cavities was observed and the number densities were about 1.0×10^{22} m^{-3}. There was no significant difference between the number densities in the different alloys, although the root mean cubes of the cavity radius are quite different for each alloy. Precipitates of the MC type were also observed in the matrix and on grain boundaries in all alloys except a high-purity (HP) ternary alloy. The JPCA-SA (including 0.06% carbon and 0.027% phosphorus) and standard type 316 steel (including 0.06% carbon and 0.028% phosphorus) showed quite low-swelling values of about 0.016 and 0.015%, respectively, while a HP ternary austenitic alloy showed the highest swelling value of 2.9%. This suggests that the existence of impurities affects the cavity growth in austenitic stainless steels even at 400°C.

PACS: 61.72

1. Introduction

The cavity density of neutron-irradiated austenitic stainless steels is known to be dependent on the He/dpa ratio [1]. Swelling is enhanced at the intermediate He/dpa ratio due to the influence of helium on the total cavity density. For small increases in the He/dpa ratio, the low-swelling transient regime (LSTR) is reduced since more helium is available to drive bubble growth to the critical size for void formation [2]. For higher He/dpa ratios, a regime can be reached in which the cavity density is so high that it begins to suppress the vacancy supersaturation. This leads to a larger critical number of gas atoms for void formation and a longer LSTR.

Most of the available swelling data of austenitic stainless steels, however, have been derived from neutron-irradiation experiments in which helium generation rates are much lower or higher than the fusion-relevant conditions. A mixed-spectrum fission reactor in which the helium generation rate and damage rate are maintained at constant level can be utilized for such a fusion-relevant experiment. Irradiation of austenitic stainless steels in a mixed-spectrum fission reactor results in the following transmutation with the thermal neutrons: $^{58}Ni(n,\gamma)^{59}Ni(n,\alpha)^{56}Fe$. The initial helium production rate is relatively low, but the amount of helium increases with irradiation dose because of the two-step transmutation reaction. Spectral tailoring by adjusting a ratio of thermal to fast neutron fluxes is a method for controlling this non-linearity in He/dpa ratio from the naturally occurring ratio of nickel

* Corresponding author. Tel.: +1-865 576 2714; fax: +1-865 574 0641.

E-mail address: hashimoton@ornl.gov (N. Hashimoto).

0022-3115/00/$ - see front matter
PII: S0022-3115(00)00046-5

Table 1
Chemical compositions of the specimens (wt%) (Balance Fe)

	Cr	Ni	Ti	Nb	Si	Mo	Mn	B	C	N	P	S
JPCA	14.2	15.6	0.24	–	0.50	2.3	1.77	0.0031	0.06	0.0039	0.027	0.005
316R	16.8	13.5	0.005	–	0.61	2.5	1.80	–	0.06	–	0.028	0.003
C	15.4	15.6	0.25	0.08	0.51	2.4	1.56	–	0.02	0.0018	0.017	0.007
K	18.0	17.6	0.29	–	0.48	2.6	1.46	–	0.02	0.0018	0.015	0.005
HP	17.1	11.8	–	–	0.005	–	–	–	0.005	0.020	–	–

Table 2
Damage levels, helium concentrations and He/dpa ratio of the type 316 and the JPCA irradiated at 400°C in spectrally tailored experiment of the ORR and the HFIR

	316			JPCA		
	dpa	appm He	He/dpa	dpa	appm He	He/dpa
ORR	7.4	100	14	7.4	155	21
HFIR	9.9	100	10	9.9	125	13
ORR + HFIR	17.3	200	12	17.3	280	16

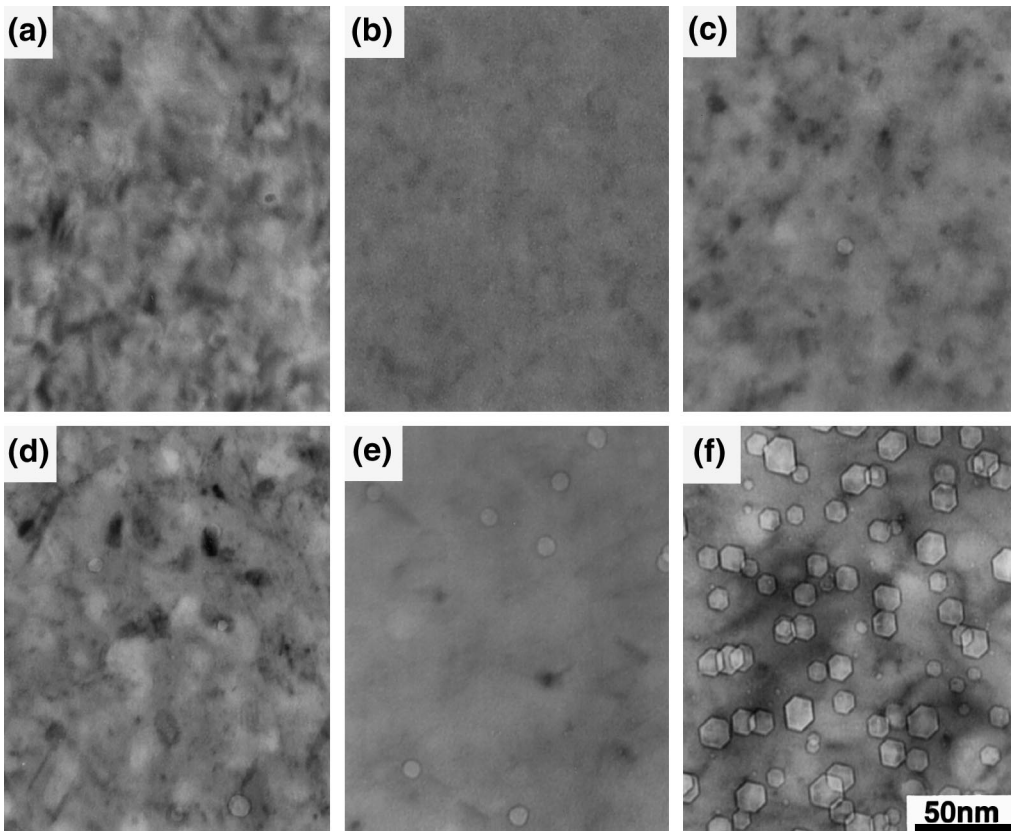

Fig. 1. Cavity microstructures of the alloys irradiated at 400°C to 17.3 dpa in spectrally tailored experiment of the ORR and the HFIR: (a) aged-JPCA, (b) JPCA-SA, (c) 316R-SA, (d) C-SA, (e) K-SA and (f) HP.

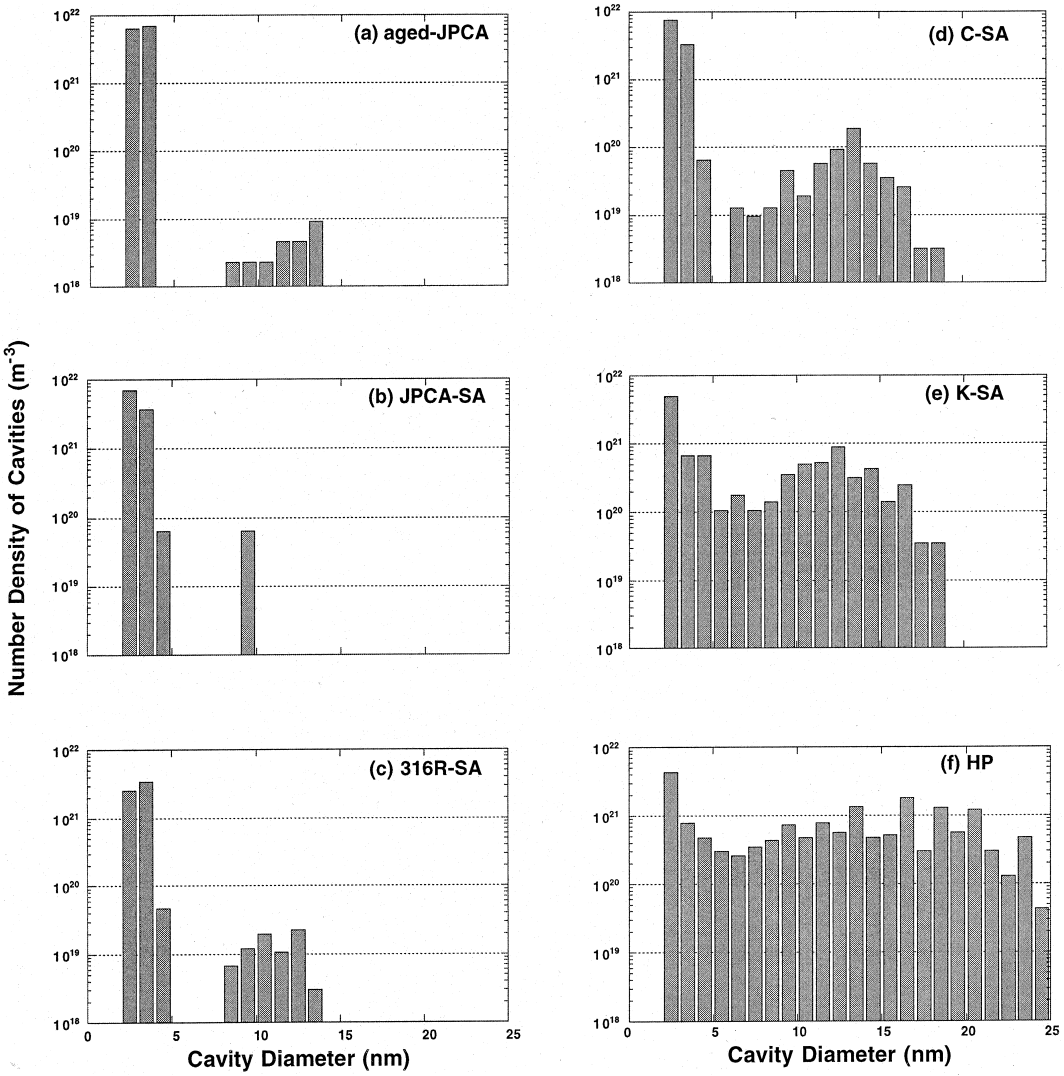

Fig. 2. Size distribution of cavities in the alloys irradiated at 400°C to 17.3 dpa in spectrally tailored experiment of the ORR and the HFIR.

Table 3
Summary of cavities observed in the alloys irradiated at 400°C to 17.3 dpa in spectrally tailored experiment of the ORR and the HFIR

	Number density (m^{-3})	Root mean cube of cavity radius (nm)	Swelling (%)
Aged-JPCA	1.7×10^{22}	1.4	0.020
JPCA-SA	1.1×10^{22}	1.5	0.016
316R-SA	6.2×10^{21}	1.8	0.015
C-SA	1.1×10^{22}	2.5	0.079
K-SA	1.0×10^{22}	4.0	0.27
HP	1.9×10^{22}	7.2	2.9

isotopes and for keeping the approximately linear He/dpa ratio close to a fusion-relevant level during the course of irradiation.

The US–Japan collaborative program for the development of fusion materials includes several spectral tailoring experiments [3–6]. The present work is a continuation of the irradiation in the ORR-MFE-7J spectrally tailored capsule. The HFIR-MFE-RB* experiments were designed for irradiation in the removable beryllium (RB*) positions of the HFIR; the capsules are surrounded by a hafnium shield in order to reduce the thermal neutron flux and achieve a He/dpa level near that expected fusion reactor [7–9]. This experiment is being conducted under the DOE/JAERI Collaborative Agreement.

2. Experimental

The austenitic stainless steels irradiated in this experiment were designated Japanese-PCA (JPCA-SA), 316R-SA, K-SA, C-SA, HP (a high-purity ternary model alloy), and aged-JPCA. The chemical compositions of the specimens used in this study are given in Table 1. The JPCA-SA contains Ti, B, and P, and has been shown resistant to swelling. The 316R-SA is a standard heat of type 316 stainless steel. The C-SA and the K-SA stainless steels have low carbon concentration, and they are exploratory alloys modified with Ti and/or Nb. The HP is a high-purity ternary alloy with Fe, Cr, and Ni contents similar to those of type 316. The JPCA-SA and the C-SA were solution-annealed at 1100°C, the 316R-SA and the K-SA were solution-annealed at 1050°C, and HP was annealed at 1200°C. The aged-JPCA was aged for 1 h at 800°C after cold-rolling ~20%.

The irradiation in the ORR produced approximately 102–125 appm He in the steels [10], giving a fusion relevant He/dpa ratio of about 11.7 appm/dpa. In JPCA, however, ^{10}B also contributes at the very early stage of irradiation, and increases the helium levels by 30 appm [3]. The final helium level in JPCA is, therefore, 155 appm. These specimens were subsequently irradiated in the HFIR-RB* positions with a hafnium shield to reduce the thermal neutron flux and so continue the irradiation at a He/dpa level near that expected in a fusion reactor. The operating temperature of the HFIR-MFE-RB*-400J-1 capsule was 400°C, with the temperature controlled by changing the gas mixture around the specimen holder. The thermal and fast ($E > 0.1$ MeV) neutron fluences in the ORR were 8.1×10^{21} and 9.5×10^{25} n/m^2, and those of the HFIR were 4.0×10^{25} and 1.6×10^{26} n/m^2, respectively [5]. The capsule achieved a fluence in the ORR of 7.4 dpa and in the HFIR of 9.9 dpa [5]. The helium content measured by isotope-dilution gas mass spectrometry [10] is given in Table 2.

Specimens for transmission electron microscopy (TEM) were thinned using an automatic Tenupol electropolishing unit in a shielded glove box. TEM disks were examined using a JEM-2000FX transmission electron microscope operated at 200 kV. The foil thicknesses were measured by thickness fringe or the improved contamination parallax method [11] in order to quantify defect density values.

3. Results

3.1. Cavities

Fig. 1 shows cavity microstructures of the alloys irradiated at 400°C to 17.3 dpa in the ORR/HFIR spectrally tailored experiment. The size distribution of cavities in all of the alloys showed bi-modal behavior, and differences between critical radii for each alloy were not significant, as shown in Fig. 2. Table 3 summarizes the cavity data for the alloys and Fig. 3 shows a comparison of number densities, root mean cube of radius and swelling of the alloys. There is no significant difference of cavity number densities for each alloy, while the root mean cube of cavity radius are quite different. Although the cavity density was similar in all the alloys, the swelling values of aged-JPCA, JPCA-SA, 316R-SA,

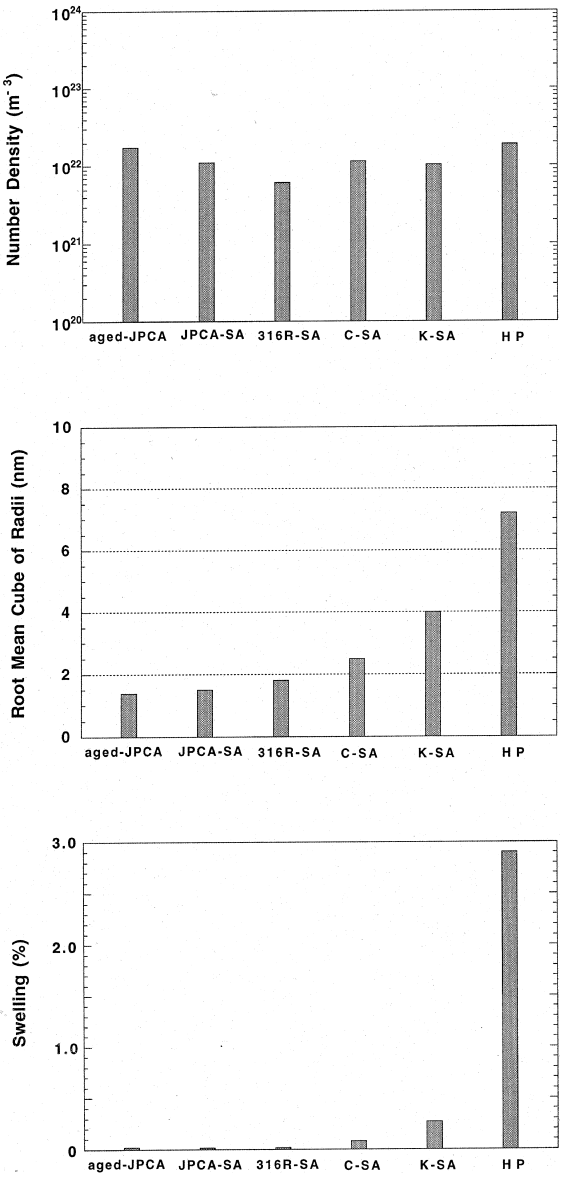

Fig. 3. Comparison of number densities, root mean cube of radius and swelling of the alloys irradiated at 400°C to 17.3 dpa in spectrally tailored experiment of the ORR and the HFIR.

C-SA and K-SA were less than 0.3%, while that of HP was about 3%.

3.2. Dislocation loop evolution

Fig. 4 shows dislocation loops in the alloys irradiated at 400°C to 17.3 dpa in the spectral tailoring experiment. The micrographs were taken with beam direction close to [0 1 1] using streaks in the diffraction pattern arising from the faulted loops. The loops observed in the alloys were Frank type faulted loops on {1 1 1} planes, which were identified by reflection from stacking faults in weak beam dark-field image. There is a tendency for higher number densities to be correlated with smaller average loop sizes, but basically there is no significant difference in number densities and total dislocation densities between the alloys. The dislocation loop data in the alloys are summarized in Table 4.

Table 4
Summary of dislocations observed in the alloys irradiated at 400°C to 17.3 dpa in spectrally tailored experiment of the ORR and the HFIR

	Number density (m^{-3})	Mean size (nm)	Total dislocation density (m^{-2})
Aged-JPCA	7.3×10^{21}	15.2	3.5×10^{14}
JPCA-SA	1.0×10^{22}	15.7	4.1×10^{14}
316R-SA	9.5×10^{21}	20.2	6.0×10^{14}
C-SA	3.3×10^{21}	26.3	2.7×10^{14}
K-SA	4.5×10^{21}	22.1	3.1×10^{14}
HP	4.0×10^{21}	27.0	3.4×10^{14}

3.3. Precipitate evolution

Fig. 5 shows the precipitates formed in the alloys irradiated at 400°C to 17.3 dpa. In all the alloys except the HP, precipitates with Moiré fringes were observed in the matrix with a high number density of about 2×10^{20}–8×10^{21} m^{-3}, as summarized in Table 5. The number density of MC in the 316R-SA was lower than that of the other titanium-containing alloys because the 316R-SA contained only 0.005% titanium. The alloys containing titanium as a swelling inhibitor were expected

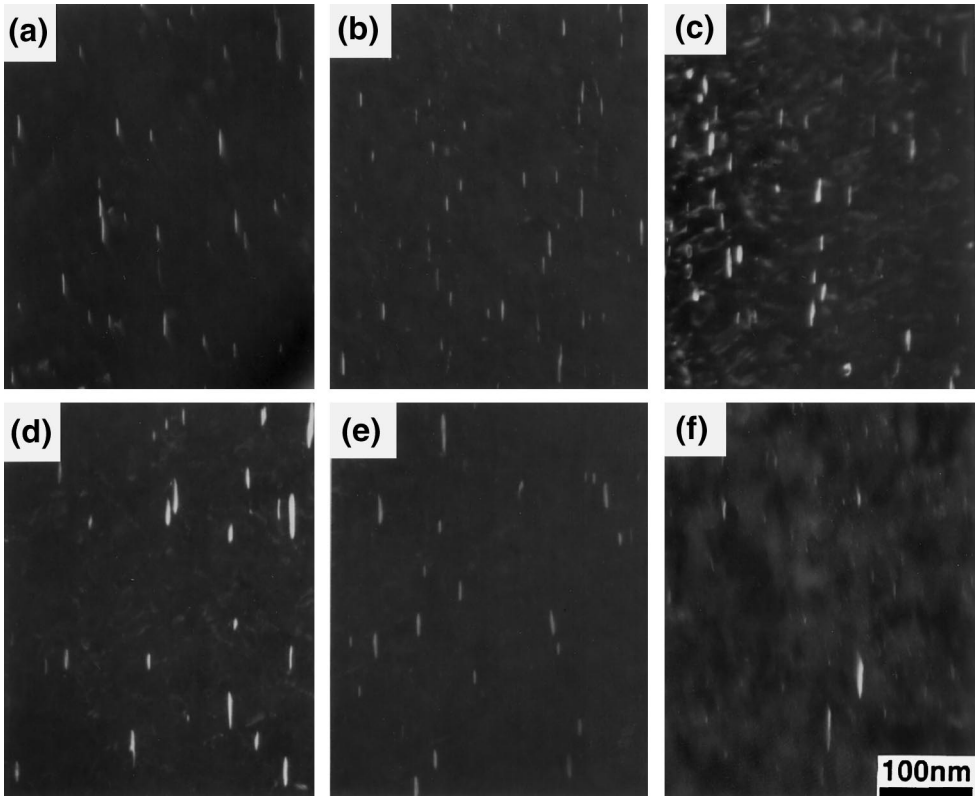

Fig. 4. Dislocation loops in the alloys irradiated at 400°C to 17.3 dpa in spectrally tailored experiment of the ORR and the HFIR. The micrographs were taken with beam direction B close to [0 1 1] using streaks in the diffraction pattern arising from the faulted loops: (a) aged-JPCA, (b) JPCA-SA, (c) 316R-SA, (d) C-SA, (e) K-SA and (f) HP.

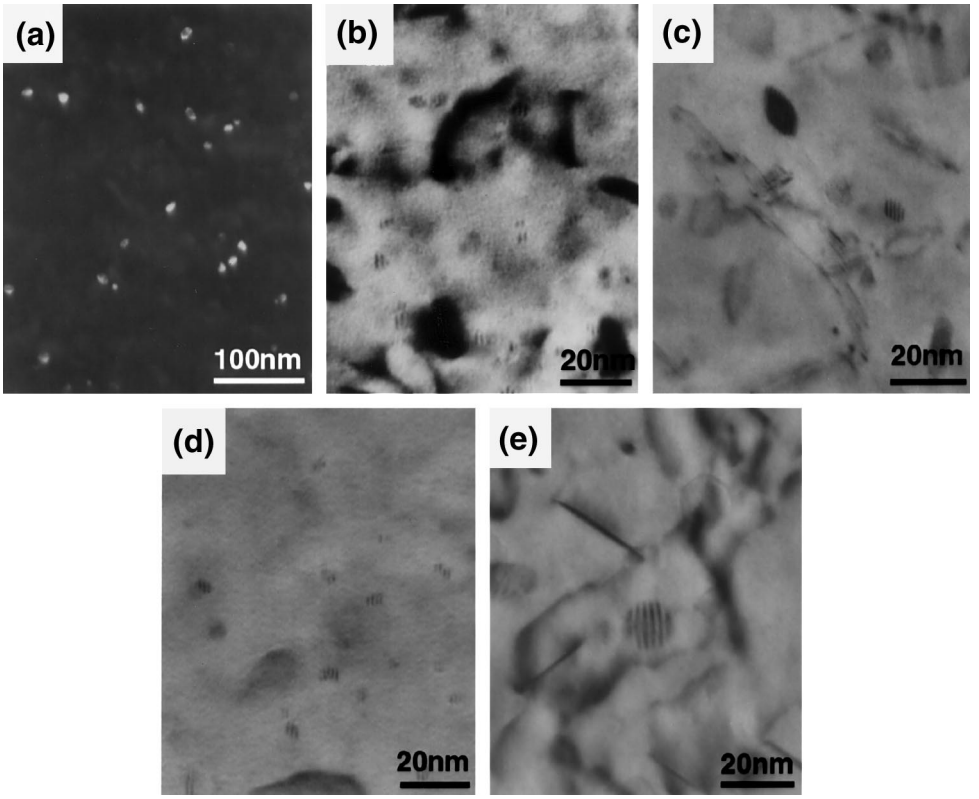

Fig. 5. MC-type precipitates formed in the alloys irradiated at 400°C to 17.3 dpa in the ORR and the HFIR: (a) aged-JPCA, (b) JPCA-SA, (c) 316R-SA, (d) C-SA and (e) K-SA.

Table 5
Summary of precipitates observed in matrix of the alloys irradiated at 400°C to 17.3 dpa in spectrally tailored experiment of the ORR and the HFIR

	Precipitates	Number density (m^{-3})	Mean size (nm)
Aged-JPCA	MC	1.3×10^{21}	11.5
	M_6C	5.1×10^{20}	10.2
JPCA-SA	MC	7.7×10^{21}	3.4
	M_6C	1.2×10^{21}	7.4
316R-SA	MC	2.0×10^{20}	7.2
	M_6C	9.1×10^{20}	7.1
C-SA	MC	5.8×10^{21}	5.3
	M_6C	4.6×10^{20}	8.5
K-SA	MC	7.1×10^{20}	18.7
	M_6C	2.4×10^{20}	19.5
HP	–	–	–

to form MC precipitates along dislocation loops and to provide effective traps for helium and mediate the cavity distribution. In this experiment, however, MC precipitates formed not along dislocation loops but in the matrix.

4. Discussion

The alloys irradiated in this spectral tailoring experiment showed different values of swelling. The cavity size distributions in the alloys showed bi-modal behavior, indicating mixed populations of smaller subcritical helium bubbles and larger bias-driven voids. There was no significant difference in the cavity number density for each alloy, while the root mean cube of the radii were quite different. This suggests that the alloy-to-alloy difference in swelling behavior is due to the differences in size distribution of cavities, especially the population of bias-driven voids. A higher growth rate of voids leads to larger swelling in the alloys.

In this experiment, the alloys except HP contained titanium as a swelling inhibitor. Titanium is expected to form MC-type precipitate along dislocations, inhibiting the preferential absorption of interstitial atoms by dislocations and modifying the distribution of helium. However, a high number density of MC precipitates exhibiting Moiré fringes were observed not along dislocations but in the matrix. Furthermore, there was no correlation between carbon content and the number density of MC precipitates or with the swelling resistance.

The void nucleation in austenitic stainless steel irradiated at high temperature has been explained on the basis of differences in the dislocation structure that evolves. A higher density of loops leads to a higher total dislocation density which reduces the vacancy supersaturation; hence, the void nucleation rate is reduced. The austenitic stainless steels irradiated in this experiment included some impurities, which would affect the density of Frank loops and cavity growth due to a change in the vacancy mobility. The effect of carbon and nitrogen concentration on microstructures were shown in Figs. 6 and 7. In the alloys including carbon, phosphorus, and silicon, there is a similar tendency for number density of Frank loops to increase and root mean cube of cavity radii to decrease with their concentration, which results in suppression of swelling (see Fig. 6). Conversely, the presence of high nitrogen (0.020%) results in large swelling with large size of cavity radii, as shown in Fig. 7.

The JPCA-SA and 316R-SA containing a large amount of carbon, phosphorus, and silicon showed relatively good swelling resistance, while C-SA and K-SA with lower amounts of these impurities showed poor swelling resistance. The HP alloy, which had less carbon, phosphorus, and silicon showed the largest swelling value. Besides, the HP alloy includes larger amount of nitrogen compared with the other alloys. Therefore, there is a possibility that the existence of nitrogen

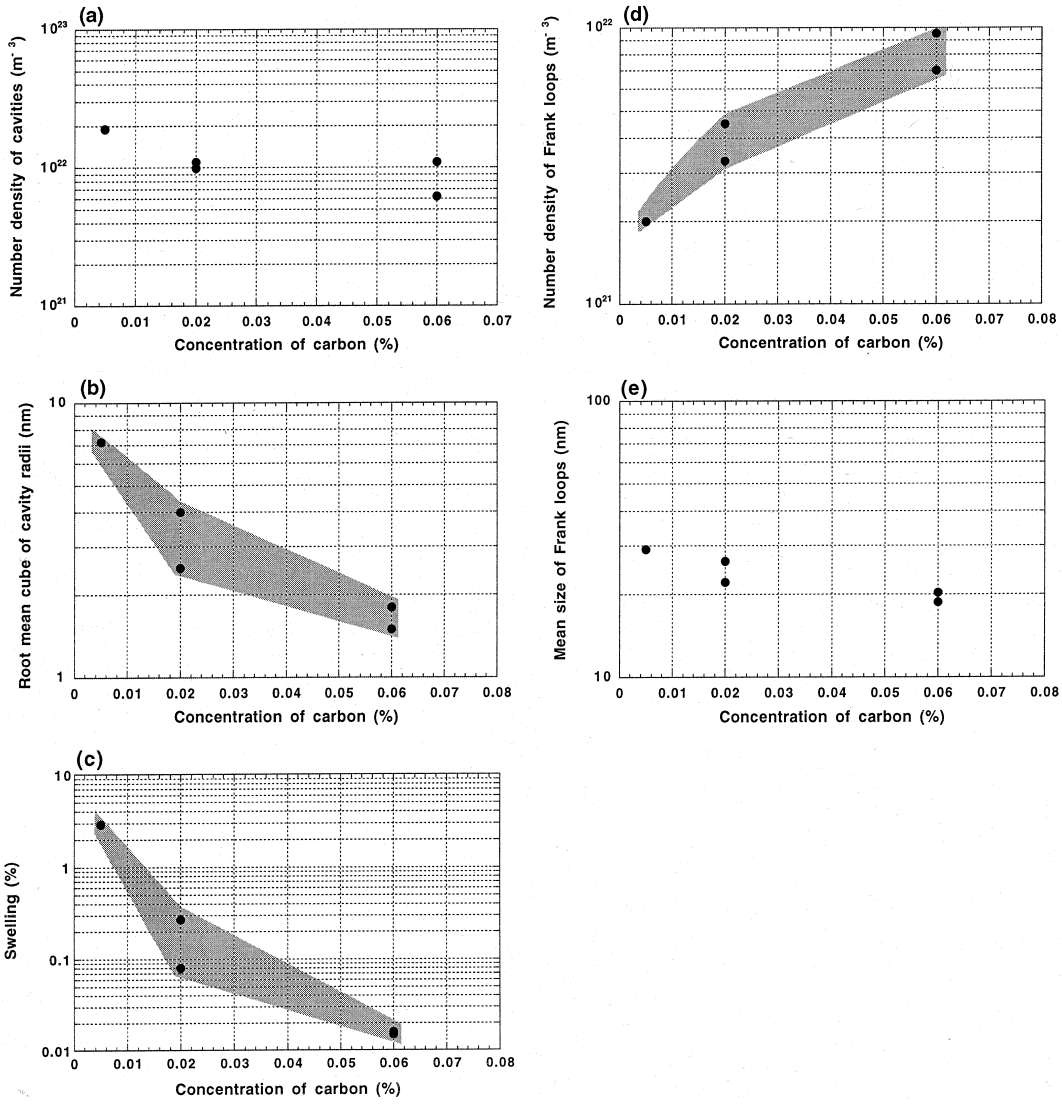

Fig. 6. The effect of carbon concentration on microstructures: (a) number density of cavities, (b) root mean cube of cavity radii, (c) swelling, (d) number density of Frank loops and (e) mean size of Frank loops.

affected the cavity growth during irradiation. The role of impurities in the void swelling of 316 stainless steel electron-irradiated at 500°C and 550°C has been investigated [12–15]; Naito et al. [12] reported that the swelling of 316 tends to decrease with the amount of carbon and increase with the amount of nitrogen. According to Lee et al. [13,14], the addition of phosphorus alone could not provide significant reduction in swelling, while in the case where phosphide precipitates are introduced, swelling would be suppressed. In this experiment, however, no phosphide formation was observed. There is a possibility of an interaction between phosphorus atoms and vacancies [15], which could result in swelling suppression. Zinkle et al. [16] pointed out that oxygen and other surface-active impurities (e.g., sulfur) could stabilize void formation through a chemisorption-induced decrease in the void surface tension. It is worth noting that the alloys except HP contained oxygen gettering elements Si and Ti, although the effect of oxygen on swelling could not be quantified in this experiment. Fig. 8 shows the dependence of impurity concentration and number density of precipitates on swelling. Swelling increased with increasing nitrogen and decreasing carbon, phosphorus, and silicon, while there was no relationship between swelling and number density of precipitates in this experiment as mentioned above.

Fig. 9 shows the dose dependence of swelling in the alloys irradiated at 400°C in the ORR/HFIR spectrally

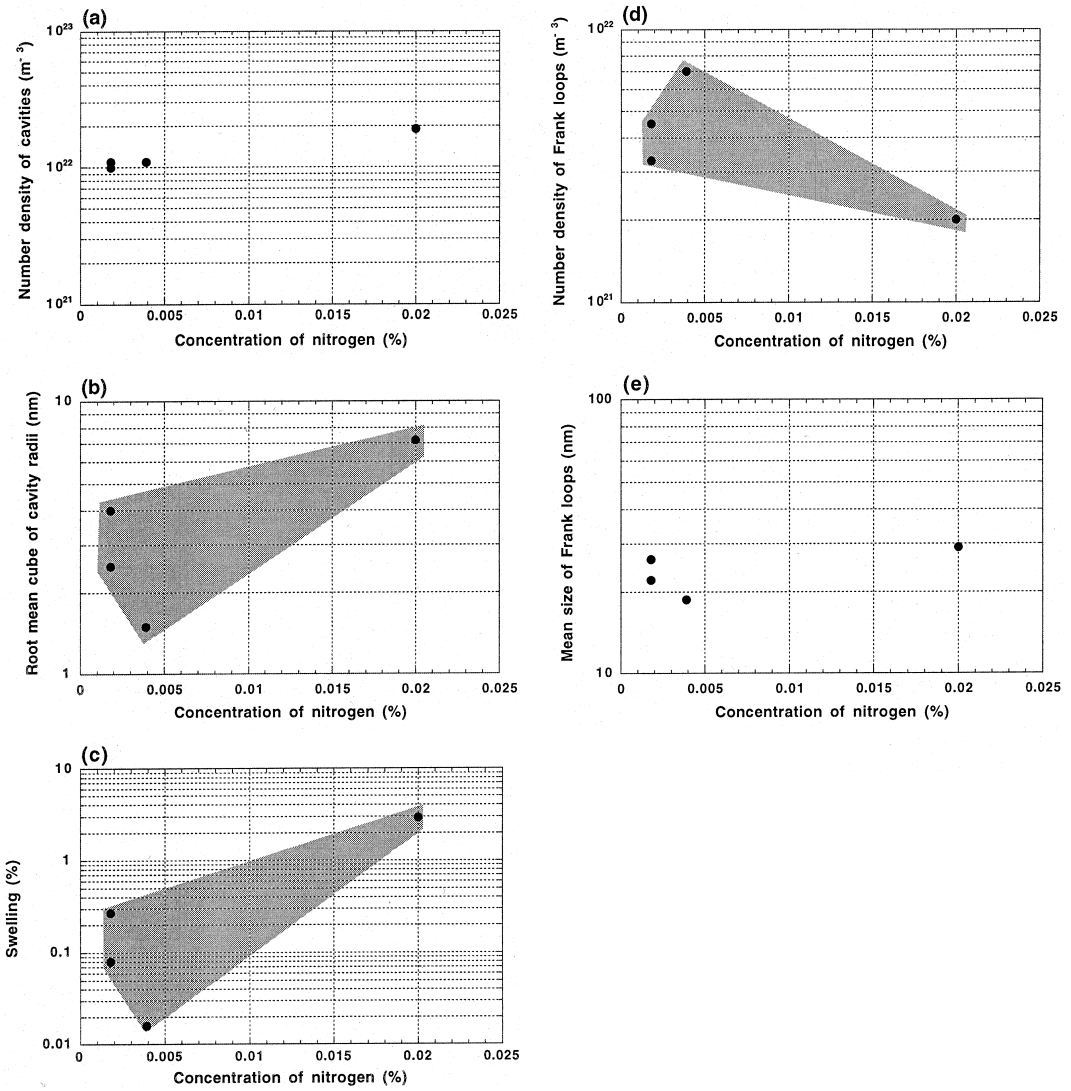

Fig. 7. The effect of nitrogen concentration on microstructures: (a) number density of cavities, (b) root mean cube of cavity radii, (c) swelling, (d) number density of Frank loops and (e) mean size of Frank loops.

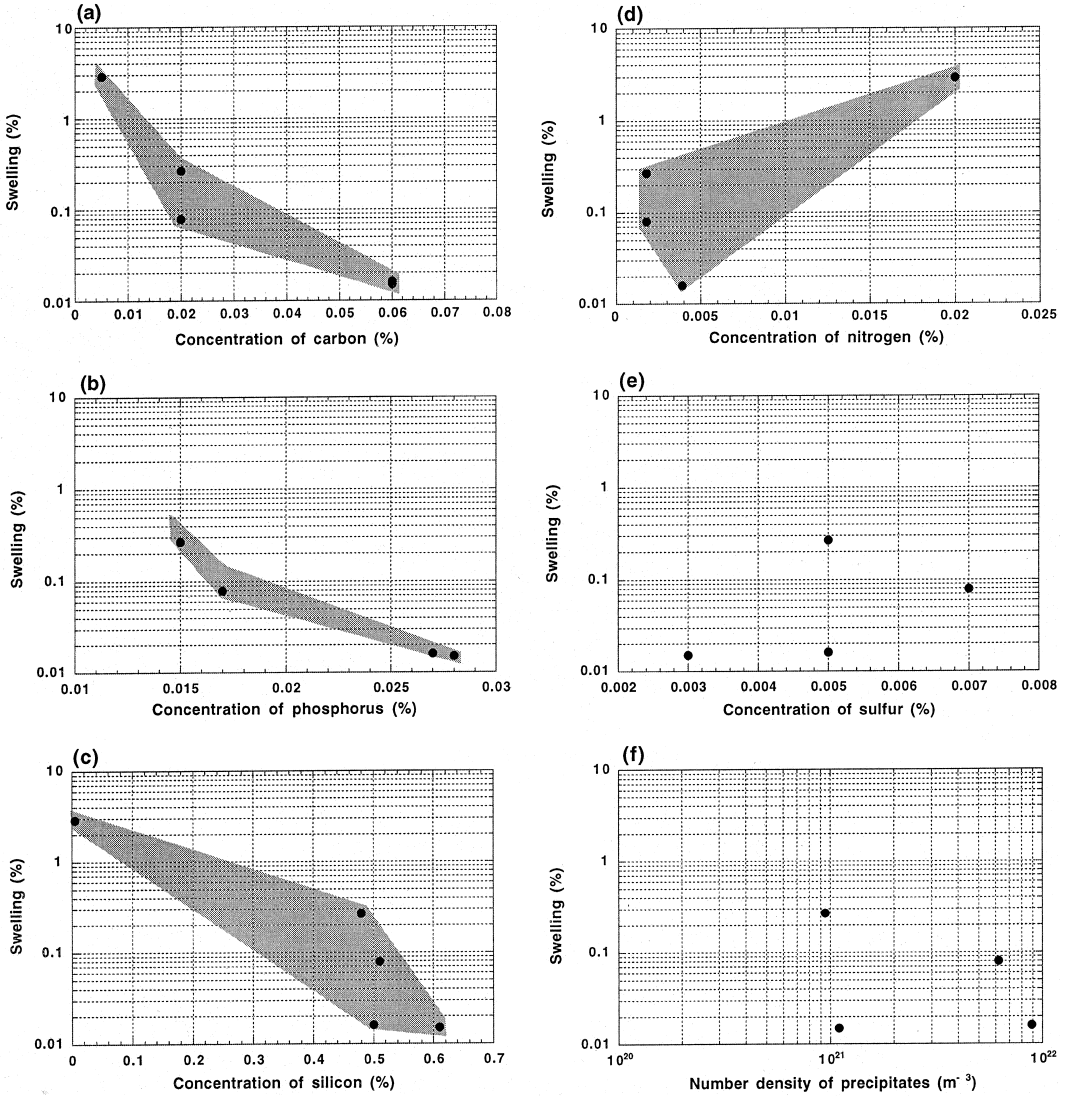

Fig. 8. The dependence of impurity concentration and number density of MC on swelling: (a) carbon, (b) phosphorus, (c) silicon, (d) nitrogen, (e) sulfur and (f) MC.

tailored experiment with some previous data at 7.4 dpa [3]. This indicates that all of the alloys except HP are still in the LSTR, while HP appears to be in the near-linear swelling rate regime (0.2% dpa^{-1}). HP would be still in transition between LSTR and steady-state swelling regime. According to a report of spectral tailoring experiment in ORR (MFE-4A/4B) [5], swelling of USPCA-SA irradiated to 13 dpa at 400°C was about 0.35%, which was in the initial LSTR. If one assumed similar irradiation response in both USPCA-SA and JPCA-SA, the swelling of JPCA-SA was expected to be about 0.3% in this experiment. JPCA-SA irradiated to 17 dpa at 400°C, however, showed below 0.02% swelling. This could be explained by the difference of impurity level in the two alloys. There is not much difference in the amount of carbon, silicon, and sulfur between the USPCA-SA and the JPCA-SA, while the JPCA-SA contains much less nitrogen and much more phosphorus compared with USPCA-SA. Therefore, the swelling resistance in JPCA-SA could be due to the effects of more phosphorus and less nitrogen, in addition to the presence of carbon and silicon.

5. Conclusions

Microstructural evolution in several kinds of austenitic stainless steel, irradiated at 400°C to 17.3 dpa in

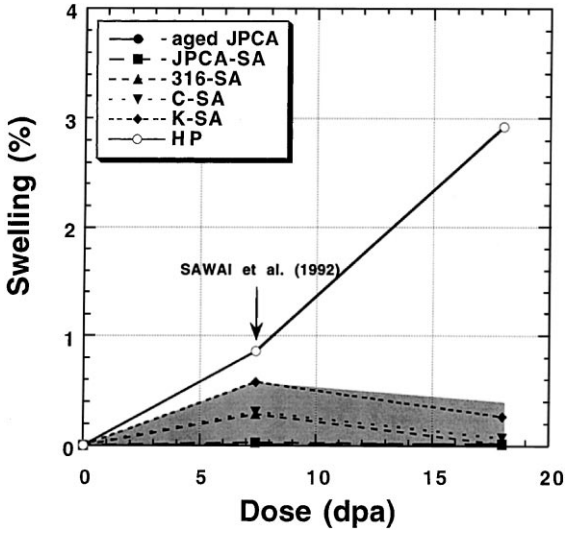

Fig. 9. Dose dependence of swelling in the alloys irradiated at 400°C in the spectrally tailored experiment. The previous data [3] are plotted at 7.4 dpa.

the ORR/HFIR spectrally tailored experiment, was investigated by TEM. The cavity distributions in the alloys showed bi-modal behavior and there was no significant difference in the cavity number densities between the alloys, while the root mean cube of the cavity radii were quite different. This suggests that the alloy-to-alloy difference in swelling behavior is due to the differences in size distribution of cavities, especially the bias-driven void population. The alloys containing variations in carbon, phosphorus, and silicon showed good swelling resistance. Conversely, the presence of nitrogen might result in large swelling. The dose has not yet exceeded the initial LSTR in this spectrally tailored experiment. This could be related to the effect of the presence of impurities, which could interact with and reduce the mobility of vacancies.

Acknowledgements

The authors would like to thank Dr A.F. Rowcliffe, Dr R.E. Stoller, Dr E.H. Lee, and Dr S.J. Zinkle for their helpful discussions. This research was supported in part by an appointment to the Oak Ridge National Laboratory Postdoctoral Research Associates Program administered jointly by the Oak Ridge Institute for Science and Education and Oak Ridge National Laboratory.

References

[1] G.R. Odette, P.J. Maziasz, J.A. Spitznagel, J. Nucl. Mater. 103&104 (1981) 1361.
[2] R.E. Stoller, G.R. Odette, Radiation induced changes in microstructure, in: F.A. Garner, N.H. Packan, A.S. Kumar (Eds.),13th Conference, ASTM STP 955, ASTM, Philadelphia, 1987, p. 358.
[3] T. Sawai, P.J. Maziasz, A. Hishinuma, J. Nucl. Mater. 179–181 (1991) 519.
[4] T. Sawai, P.J. Maziasz, H. Kanazawa, A. Hishinuma, J. Nucl. Mater. 191–194 (1992) 712.
[5] J.P. Robertson, I. Ioka, A.F. Rowcliffe, M.L. Grossbeck, S. Jitsukawa, in: R.K. Nanstad et al. (Eds.), 18th International Symposium, ASTM STP1325, American Society for Testing and Materials, Philadelphia, 1997.
[6] E. Wakai, N. Hashimoto, J.P. Robertson, S. Jitsukawa, T. Sawai, A. Hishinuma, Tensile properties and damage microstructures in ORR/HFIR-irradiated austenitic stainless steels, in: Proceedings of 9th Int. Conf. on Fusion Reactor Materials (ICFRM-9), J. Non-Cryst. Solids (2000) in press.
[7] M.L. Grossbeck et al., in: Proceedings of the Conference on Fast, Thermal, and Fusion Reactor Experiments, vol. 1, Salt Lake City, Utah, April 1985, p. 199.
[8] A.F. Rowcliffe, A. Hishinuma, M.L. Grossbeck, S. Jitsukawa, J. Nucl. Mater. 179–181 (1991) 125.
[9] R.E. Stoller, P.J. Maziasz, A.F. Rowcliffe, M.P. Tanaka, J. Nucl. Mater. 155–157 (1988) 1328.
[10] L.R. Greenwood, Fusion Reactor Materials Semiannual Progress Report, 31 March 1989, DOE/ER-0313/6, US-DOE, Office of Fusion Energy, p. 23.
[11] T. Sawai, M. Suzuki, P.J. Maziasz, A. Hishinuma, J. Nucl. Mater. 187 (1992) 146.
[12] A. Naito, N. Eguchi, E. Nishibe, H. Saikawa, N. Igata, in: A. Kohama, H. Matsui, S. Tanaka, H. Takahashi (Eds.), JCSTEA 7 Series Symposium, Materials for Advance Energy System and Fission and Fusion Engineering, vol. 94, p. 374.
[13] E.H. Lee, L.K. Mansur, J. Nucl. Mater. 141–143 (1986) 695.
[14] E.H. Lee, L.K. Mansur, Metall. Trans. A 23 (1992) 1977.
[15] A.F. Rowcliffe, R.B. Nicholson, Acta. Metall. 20 (1972) 143.
[16] S.J. Zinkle, E.H. Lee, Metall. Trans. A 21 (1990) 1037.